Title	Development of a one-dimensional Wolter mirror for achromatic full-field X-ray microscopy
Author(s)	Matsuyama, S.; Kidani, N.; Mimura, H. et al.
Citation	Proceedings of SPIE - The International Society for Optical Engineering. 2011, 8139, p. 813905
Version Type	VoR
URL	https://hdl.handle.net/11094/86991
rights	Copyright 2011 Society of Photo-Optical Instrumentation Engineers (SPIE). Downloading of the abstract is permitted for personal use only.
Note	

Development of a one-dimensional Wolter mirror
for achromatic full-field X-ray microscopy

S. Matsuyama*[a,b], N. Kidani[a], H. Mimura[c], J. Kim[a], Y. Sano[a], K. Tamasaku[d], Y. Kohmura[d],
M. Yabashi[d], T. Ishikawa[d], K. Yamauchi[a,b]

[a] Department of Precision Science and Technology, Graduate School of Engineering,
Osaka University, 2-1 Yamada-oka, Suita, Osaka 565-0871, Japan
[b] Research Center for Ultra-Precision Science and Technology, Graduate School of Engineering,
Osaka University, 2-1 Yamada-oka, Suita, Osaka 565-0871, Japan
[c] Department of Precision Engineering, School of Engineering ,
The University of Tokyo, 7-3-1 Hongo, Bunkyoku, Tokyo 113-8656, Japan
[d] RIKEN/SPring-8, 1-1-1 Kouto, Sayo-cho, Sayo-gun, Hyogo 679-5148, Japan

ABSTRACT

We investigated a one-dimensional Wolter mirror (which consists of an elliptical mirror and a hyperbolic mirror) with the aim of developing an achromatic full-field X-ray microscope with a resolution of better than 50 nm. X-ray mirrors were ultraprecisely fabricated by elastic emission machining to give a figure accuracy of 2 nm (peak-to-valley). A one-dimensional Wolter mirror that had been precisely constructed was evaluated in terms of the point-spread function at the center of the field of view (FOV) and the FOV at an X-ray energy of 11.5 keV at BL29XUL of SPring-8. It was found to have a minimum resolution of 43 nm and a FOV equivalent to 12.1 μm. These results are highly consistent with calculation results.

Keywords: advanced Kirkpatrick–Baez mirrors, Wolter mirror, full-field X-ray microscopy, X-ray mirror

1. INTRODUCTION

Microscopy has historically been used to open up new scientific frontiers. Considerable effort has gone into developing novel microscopies. X-ray microscopy has recently been attracting interest due to its potential to realize high spatial resolutions (comparable to those of electron microscopy) and its high penetration, which enables relatively thick (> 10 μm) samples and samples in special environments (e.g., aqueous solutions and gaseous atmospheres) to be observed. Moreover, a key advantage of X-ray microscopy is that X-ray analysis can be simultaneously performed to obtain additional information. For example, X-ray fluorescence imaging can be used to observe elemental distributions in real time. In addition, when used in combination with X-ray absorption spectroscopy, X-ray microscopy is a potentially powerful tool for imaging chemical state distributions. X-ray microscopy with such analysis capability and sub-50-nm resolution is expected to be used in various scientific fields.

Realizing such X-ray microscopy necessitates developing achromatic imaging optics. We have studied advanced Kirkpatrick–Baez (AKB) mirror optics[1–3] (see Fig. 1) with the aim of developing achromatic full-field X-ray microscopy with a sub-50-nm resolution. AKB mirrors consist of two pairs of an elliptical mirror and a hyperbolic mirror [i.e., two pairs of one-dimensional (1D) Wolter mirrors] that are aligned perpendicularly to each other, as in Kirkpatrick–Baez mirrors[4]. Total-reflection X-ray mirrors do not suffer from chromatism because total reflection is almost independent of wavelength. AKB mirrors have the potential to be used to realize high-resolution X-ray microscopy because it is relatively straightforward to figure nearly planar mirrors and it prevents degradation of the spatial resolution. In the present study, which represents a first step in our research, we fabricated a 1D Wolter mirror consisting of an elliptical mirror and a hyperbolic mirror and we investigated it to demonstrate the feasibility of AKB mirrors.

1D imaging tests were performed at an X-ray energy of 11.5 keV at BL29XUL[5] of SPring-8. The point-spread function (PSF) at the center of the field of view (FOV) was evaluated. The FOV was investigated by obtaining a series of PSFs

* matsuyama@prec.eng.osaka-u.ac.jp; phone/fax +81-6-6879-7286; http://www.dma.jim.osaka-u.ac.jp/kg-portal/aspi/RX0011D.asp?UNO=16683
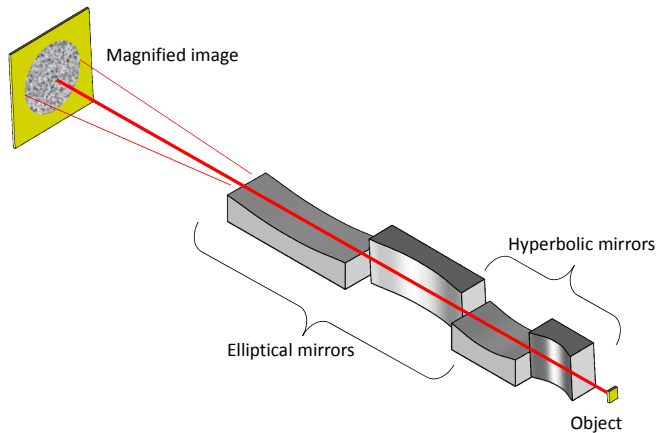
Figure 1 Configuration of AKB mirrors. (This paper discusses only a one-dimensional Wolter mirror near the object.)

throughout the FOV. The minimum resolution was found to be 43 nm [full width at half maximum (FWHM)] and the FOV was 12.1 μm. This means that the two mirrors function as an optical imaging system with the expected performance.

2. ONE-DIMENSIONAL WOLTER MIRROR

2.1 Optical system

The two elliptical profiles and the two hyperbolic profiles in the AKB mirrors were optimally designed under the following conditions: the microscope has a diffraction-limited spatial resolution with a FWHM of less than 45 nm and a working distance of 50 mm. It can effectively form an image between the first and second experimental hutches at BL29XUL[5] of SPring-8 at an X-ray energy of 11.5 keV. In this case, 12 parameters were determined, including the mirror lengths, incident glancing angles, and focal lengths of the four mirrors. Table 1 lists the parameters of the two mirrors discussed in this paper and Fig. 2 illustrates the geometrical arrangement used. The optical setup, which is a demagnifying imaging system, was employed to evaluate the PSF of the 1D Wolter mirror in this study.

Table 1 Parameters of designed elliptical and hyperbolic mirrors

	Elliptical mirror	Hyperbolic mirror
a (m)[*]	22.75	10.84×10^{-3}
b (m)[*]	58.46×10^{-3}	0.5437×10^{-3}
Effective mirror length (mm)	125	29
Incident glancing angle at center (mrad)	2.8	5.0
Distance from source (m)[**]	45.17	45.32
Distance from focal point (mm)[**]	215	65
Working distance (mm)	50	
Diffraction-limited FWHM (nm)[***]	43	

[*]Elliptical mirror: $x^2/a^2 + y^2/b^2 = 1$; hyperbolic mirror: $x^2/a^2 - y^2/b^2 = 1$
[**]Distance from each point to center of the mirror
[***]At an X-ray energy of 11.5 keV

2.2 Fabrication of aspherical mirrors

The mirror substrates (synthetic silica) were roughly prefigured by the bent polishing method[6]. They were then finely corrected by numerically controlled elastic emission machining (NC-EEM)[7,8] using microstitching interferometry (MSI)[9] and relative angle determinable stitching interferometry (RADSI)[10] as figure profilers to measure the residual figure errors until they had a figure accuracy of better than 2 nm (peak-to-valley) (Fig. 3) and a smoothness of better than 0.2 nm (root mean square [RMS]) over an area of 64×48 μm^2 (Fig. 4). The figured mirrors were coated with a thin chrome binder layer and a 30-nm-thick platinum layer using a magnetron sputtering system[11]. The PSF was calculated using a wave-optical simulator[12,13]; the expected minimum resolution was estimated to be 43 nm (FWHM) and the figure errors were found to be sufficiently small (data not shown).
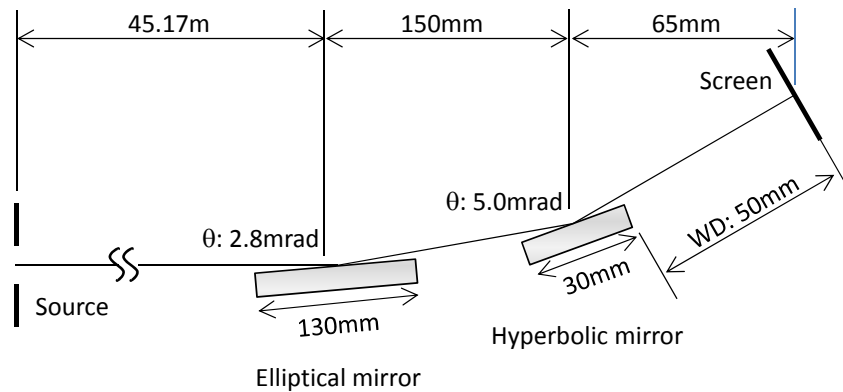
Figure 2 Geometrical arrangement of the designed 1D Wolter mirror. It can form a demagnified image of the slit on the screen.
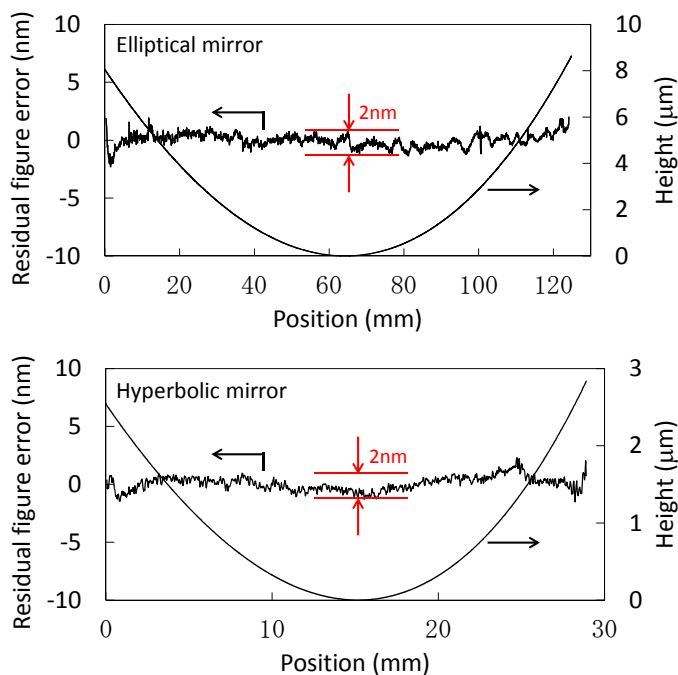

Figure 3 Mirror figures and residual figure errors on the mirror surfaces. Figured mirrors have residual figure errors of 2 nm (peak-to-valley).
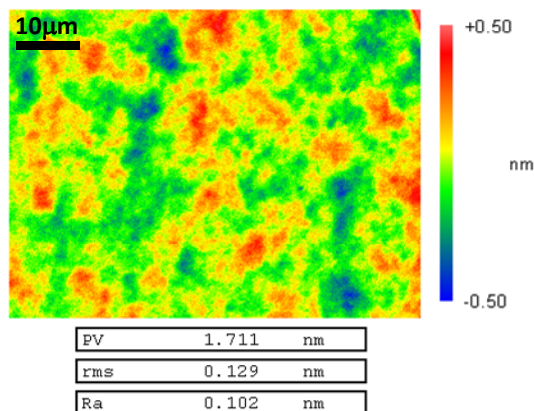

Figure 4 Surface profile of the shorter mirror measured by a phase-shift interference microscope (Zygo, New View 200CHR). After spherical correction, a surface roughness of 0.129 nm RMS over an area of 64×48 µm² was obtained.
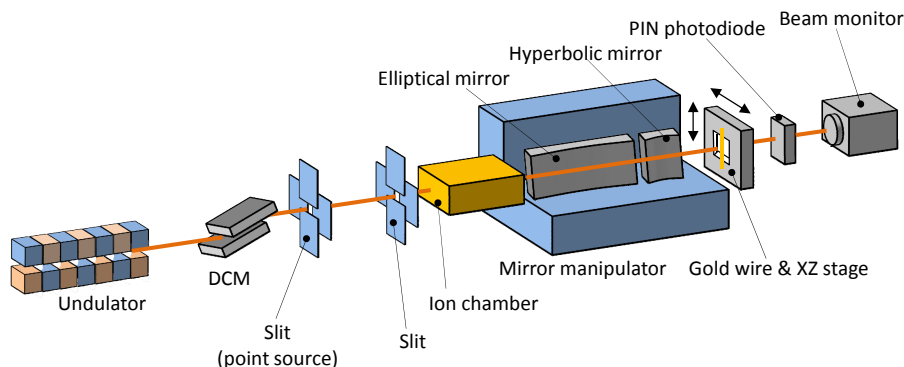
Figure 5 Experimental setup used to form a demagnified image between the first and second experimental hutches at BL29XUL of SPring-8. The upstream slit is the object of the imaging system.

3. EXPERIMENTAL SETUP

3.1 Experimental setup

Figure 5 shows a schematic of the experimental setup that was installed at BL29XUL of SPring-8. The shape of the demagnification image of the one-dimensional slit was evaluated by the wire scanning method using a 200-μm-diameter gold wire and an XZ stage (Sigma Tech, FS-1050SPXY) with a positioning resolution of 1 nm. The slit size was set to 10 μm to produce a point source for the imaging system; this size was sufficiently small to function as a point source. X-rays generated by a standard undulator at SPring-8 were monochromatized ($\Delta E/E \approx 1.4 \times 10^{-4}$ at 11.5 keV) by a double-crystal (Si(111)) monochromator (DCM). The undulator and the DCM were set to produce 11.5-keV X-rays. The second slit was installed immediately upstream of the mirrors to block X-rays incident on the outer regions of the mirror. The mirrors were installed on a specially developed mirror manipulator that enabled all the degrees of freedom of the mirrors to be adjusted. A PIN photodiode was used to detect transmitted X-rays. An ion chamber was installed immediately upstream of the mirrors to enable the results to be normalized using the incident X-ray flux. A beam monitor was used to evaluate the shape and position of reflected X-rays to roughly align the two mirrors.

3.2 Alignment method

The two mirrors were aligned based on a simple profiler, which consists of an autocollimator, a laser displacement meter, and a scanning stage. The autocollimator and displacement meter were set on the stage to obtain distributions of the slope and height of the mirrors. The system was calibrated in advance using a glass block with a flatness of less than 600 nm. As a result, the system could monitor alignment with accuracies of 1 μm and 20 μrad. Using this system, the positions of the two mirrors could be adjusted using the mirror manipulator beside the beamline. After off-line alignment, the optical system and the optical base were moved to the second experimental hutch and fine alignment of the 1D Wolter mirror was performed, especially of the incident glancing angle and the focal length, by obtaining PSFs while keeping the relative positions of the two mirrors constant.

4. RESULTS AND DISCUSSION

Experiments were performed at an X-ray energy of 11.5 keV. The shape of the demagnified image of the slit was measured by the wire scanning method. Figure 6 shows the shape obtained together with an image formed by just the elliptical mirror, which was acquired immediately after performing the imaging test of the 1D Wolter mirror by removing the hyperbolic mirror while keeping the other conditions the same. The FWHMs of both profiles agree well with the diffraction-limited values (43 and 88 nm for the 1D Wolter and elliptical mirrors, respectively). We then investigated the FOV by measuring the FWHM by the same method at various glancing incident angles of the 1D Wolter mirror. Figure 7 shows the results. For comparison, the FOV of just the elliptical mirror was also evaluated and plotted in the same way. The results show that the FOV of the 1D Wolter mirror is much wider than that of the elliptical mirror. The FOV is 12.1 μm, which agrees well with the calculated value (12.1 μm). These results reveal that the two mirrors function almost perfectly as imaging optics. This good performance is the result of both the ultraprecise fabrication and ultrafine adjustment of the mirrors. In our previous study[14], fine adjustment of the mirrors was a problem that needed to

be overcome. In the present study, we established a procedure for aligning a 1D Wolter mirror that resulted in good performance. This procedure can be applied to AKB mirrors. We expect to be able to develop AKB mirrors by adding other mirrors using the same approach.

Finally, we investigated the stability of the optical system. Figure 8 shows images formed immediately after and 5 h after the FOV tests later (nothing was done during the 5 h). Although the shape did not change, the image or wire position was shifted by only 140 nm due to thermal drift. This result is reasonable when it is considered that the experimental hutch temperature was not actively controlled; consequently, it varied by about 0.5 K. Introducing a temperature control system that can maintain the room temperature to within at least ±0.1 K should permit images to be stably acquired over periods of several hours.

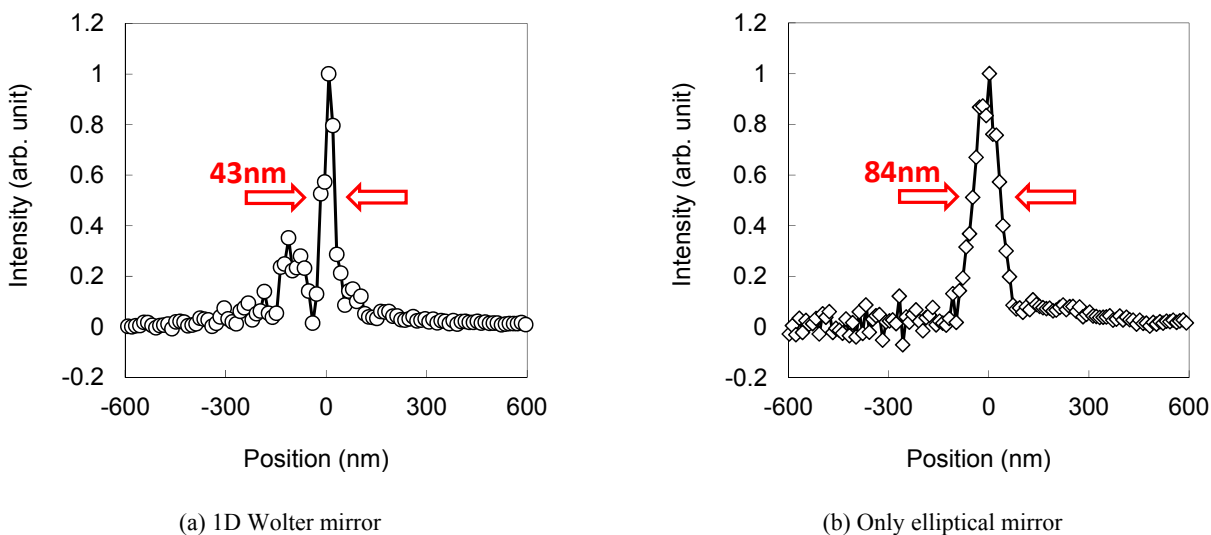(a) 1D Wolter mirror   (b) Only elliptical mirror

Figure 6 (a) Image shape formed by 1D Wolter mirror and (b) by just the elliptical mirror. Measurements were performed under the same conditions using the wire scanning method.
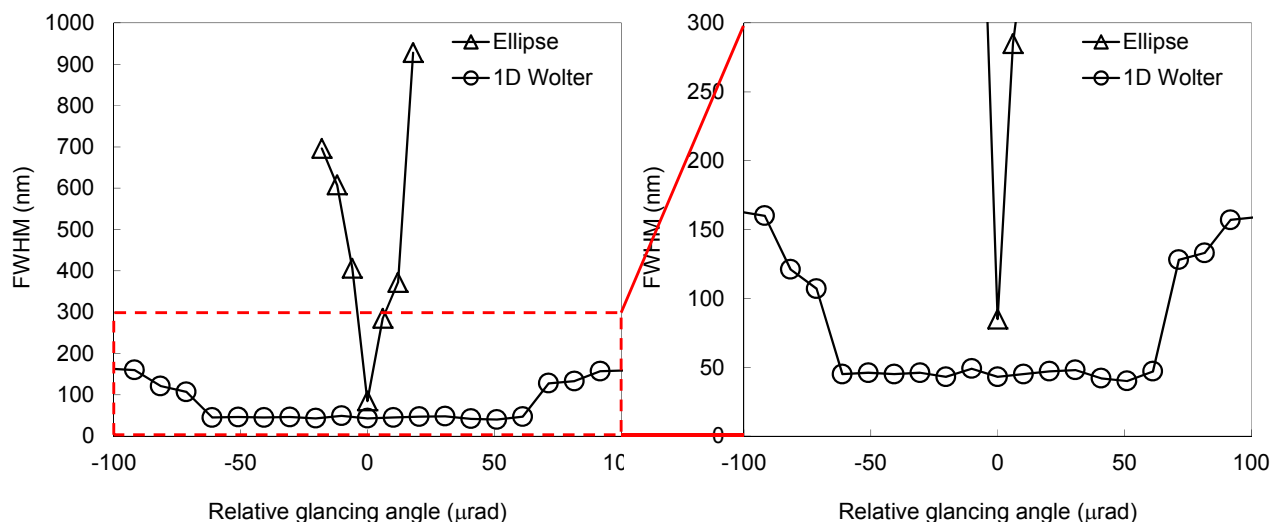

Figure 7 FOV of 1D Wolter mirror (circles) and elliptical mirror (triangles). The plot on the right is a magnified plot of the area indicated by the dashed line in the plot on the left. The horizontal axis represents the relative incident glancing angle, which is proportional to the FOV; a glancing angle of 100 µrad corresponds to a FOV of approximately 9.9 µm.
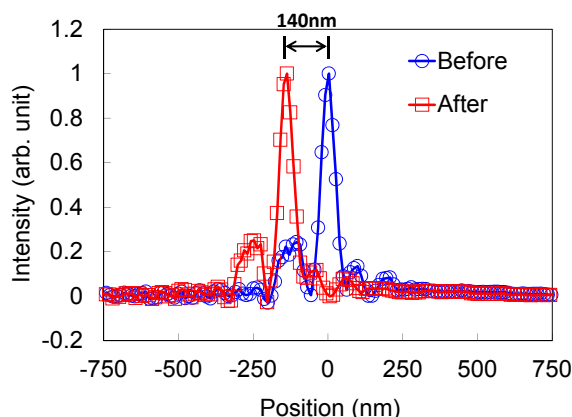
Figure 8 Evaluation of the stability of formed images. The two images were acquired under the same conditions immediately after and 5 h after the FOV tests. The image or wire position was shifted by only 140 nm due to thermal drift. The profile remained unchanged.

5. SUMMARY

A 1D Wolter mirror consisting of an elliptical mirror and a hyperbolic mirror was designed and constructed. The best spatial resolution obtained in this study was 43 nm, which is consistent with the diffraction-limited resolution and is the smallest resolution reported for Wolter mirrors. In addition, the 1D Wolter mirror had a FOV of 12.1 μm.

In the future, we intend to construct AKB mirrors by adding two other mirrors and to develop an achromatic full-field microscope with a sub-50-nm resolution. Our goal is to develop a full-field X-ray fluorescence microscope for visualizing elemental distributions. Such a microscope will be a powerful tool for imaging elemental distributions in real time. In addition, when this microscope is used in conjunction with an X-ray free electron laser with high-intensity ultrashort hard X-ray pulses it should be possible to image luminescence phenomena on a femtosecond time scale.

ACKNOWLEDGEMENTS

REFERENCES

[1] H. Wolter, "Glancing Incidence Mirror Systems as Imaging Optics for X-rays", Ann. Phys. 10, 94-114 (1952).
[2] R. Kodama et al., "Development of an advanced Kirkpatrick-Baez microscope", Optics Letters 21, 1321-1323 (1996).
[3] S. Matsuyama et al., "One-dimensional Wolter optics with a sub-50 nm spatial resolution", Optics Letters 35, 3583-3585 (2010).
[4] P. Kirkpatrick, A.V. Baez, "Formation of Optical Images by X-Rays", J. Opt. Soc. Am. 38, 766-774 (1948).
[5] K. Tamasaku et al., "Pring-8 RIKEN beamline III for coherent X-ray optics", Nucl. Instrum. Methods 467, 686-689 (2001).
[6] A. Takeuchi et al., "Kirkpatrick-Baez type x-ray focusing mirror fabricated by the bent-polishing method", Rev. Sci. Instrum. 76, 093708 (2005).
[7] K. Yamauchi et al., "Figuring with subnanometer-level accuracy by numerically controlled elastic emission machining", Rev. Sci. Instrum. 73, 4028-4033 (2002).
[8] K. Yamamura et al., "Fabrication of elliptical mirror at nanometer-level accuracy for hard x-ray focusing by numerically controlled plasma chemical vaporization machining", Rev. Sci. Instrum. 74, 4549-4553 (2003).

[9] K. Yamauchi et al., "Microstitching interferometry for x-ray reflective optics", Rev. Sci. Instrum. 74, 2894-2898 (2003).

[10] H. Mimura et al., "Relative angle determinable stitching interferometry for hard X-ray reflective optics", Rev. Sci. Instrum. 76, 045102 (2005).

[11] S. Handa, et al., "Highly accurate differential deposition for X-ray reflective optics", Surf. Interface Anal. 40, 1019-1022 (2008).

[12] K. Yamauchi et al., "Wave-optical evaluation of interference fringes and wavefront phase in hard X-ray beam totally reflected by mirror optics", Appl. Opt. 44, 6927-6932 (2005).

[13] S. Matsuyama et al., "Simulation study of four-mirror alignment of advanced Kirkpatrick-Baez optics", Nucl. Instrum. Methods 616, 241-245 (2010).

[14] S. Matsuyama et al., "Development of a one-dimensional Wolter mirror for an advanced Kirkpatrick-Baez mirror", Proc. SPIE 7802, 780202 (2010).